# APPLIED DYNAMICAL SYSTEMS

# BASIC DYNAMICAL SYSTEMS: intermittency and autocorrelation

*Lecture Notes for Classes 1–5*

**David Arrowsmith**

## Dynamical systems theory of deterministic transport *(Lectures 5–10)*

**Rainer Klages**

School of Mathematical Sciences
Queen Mary, University of London

March 16, 2009

# Chapter 1

# Basic dynamical systems and intermittency

## 1.1 Maps of the interval

We consider in this course some basic connections between iteration of maps as dynamical systems which exhibit intermittency, binary sequences and their autocorrelation properties. The study of interactions are required to develop various models with physical characteristics. For example, the study of packet traffic on communication networks requires the production of streams of binary data with so-called *long range dependence* (LRD), i.e. correlation over long ranges of sequences in the data. To take the example further - the basic requirement of a packet traffic model is to produce sequences or strings of binary digits which represent the two types of packets, those which contain information which we represent by the symbol '1' and those that are empty which are represented by '0'.

The mechanism for producing the binary strings has to be flexible and satisfy two key requirements.

- all possible data strings of a given finite length need to be realized and,
- the required statistical nature of the binary data strings should be reflected in the output for a "typical orbit" of the dynamical system.

This application driven problem allows us to address ceratin aspects of a phenomenon called **intermittency**. in this chapter by showing how iterating certain types of interval map can satisfy the statistical requirements of LRD behaviour.

An interval map is simply a function $f : \mathbb{I} \to \mathbb{I}$, where $\mathbb{I} = [0, 1] = \{x | 0 \leq x \leq 1\}$, is the closed interval of real numbers. Thus repeated iteration of the map given an initial point $x_0 \in I$ provides a sequence of real numbers $\{x_n\}$ in the interval $\mathbb{I}$ where $x_{n+1} = f(x_n)$, for $n = 0, 1, 2, \ldots$. The real

sequence can easily be turned into a binary sequence with the use of an *output* map $s : \mathbb{I} \to \{0, 1\}$ defined by

$$s(x) = \begin{cases} 0 & 0 \leq x < \bar{d} \\ 1 & \bar{d} \leq x \leq 1 \end{cases}$$

where the discriminator $\bar{d} \in (0, 1)$. Thus, given an initial $x_0 \in \mathbb{I}$, we obtain the *real* sequence $\{x_n\}$ in $\mathbb{I}$ and deduce the output *binary* sequence $\{y_n\} \subseteq \{0, 1\}^\infty$, where $y_n = s(x_n)$. Some examples of maps $f : \mathbb{I} \to \mathbb{I}$ are illustrated in Fig. 1.1.

*Remark* The monotonic functions (a), (b) in Fig. 1.1, have orbits with predictable asymptotics and so the possible corresponding binary output from such a map is severely restricted.

A geometrical interpretation of the iteration of a map can be obtained by using the *orbit web*. The sequence of points $(x_n, x_{n+1})$ gives the dynamical iteration of the orbit $x_0$. It is obtained geometrically using the symmetry line $L : y = x$ to transfer the value $y = x_{n+1} = f(x_n)$, on $gr(f)$, from the $y$-axis to the $x$-axis. This facilitates the next iteration of $f$ to give the point $x_{n+2} = f(x_{n+1})$ and so on. Thus the "web" in $\mathbb{I} \times \mathbb{I}$ is obtained by alternately filling in vertical segments from $(x_n, x_n)$ on $L$ to $(x_n, x_{n+1})$ on $gr(f)$ followed by horizontal segments from $(x_n, x_{n+1})$ to $(x_{n+1}, x_{n+1})$. This procedure alternates between points on $L$ and points on the graph of $f$ and gradually unfolds the nature of an orbit as in Fig. 1.2

## 1.2 Behaviour of orbits

A natural question to ask is what types of orbit can arise from functions such as those illustrated in Fig. 1.1.

If the graphs $y = x$ and $y = f(x)$ intersect at a point $x = x^*$, then we have a *fixed point* of the iteration, i.e. $x^* = f(x^*)$ - there is no change in the iterated value. One can then ask about the behaviour of orbits which arise in the neighbourhood of the fixed point. Such orbits can move towards or away from the fixed point becoming an *attractor*, or *repellor*, respectively. *Neutral* fixed points can also arise where orbits from one side of $x^*$ move towards the fixed point while they move away on the side. Various configurations of fixed points can be seen in Fig. 1.3. They depend on the nature of the graph $y = f(x)$ in the neighbourhood of its intersection with the 'fixed point' line. If the map is differentiable then the behaviour at a fixed point can be categorized in terms of the derivative of $f$ at the fixed point $x = x^*$. A Taylor expansion of the map $f$ in the neighbourhood $x = x^*$ gives

$$f(x) \approx f(x^*) + f'(x^*)(x - x^*), \tag{1.1}$$

and so

$$|x_{n+1} - x^*| \approx |f'(x^*)||(x_n - x^*)|. \tag{1.2}$$

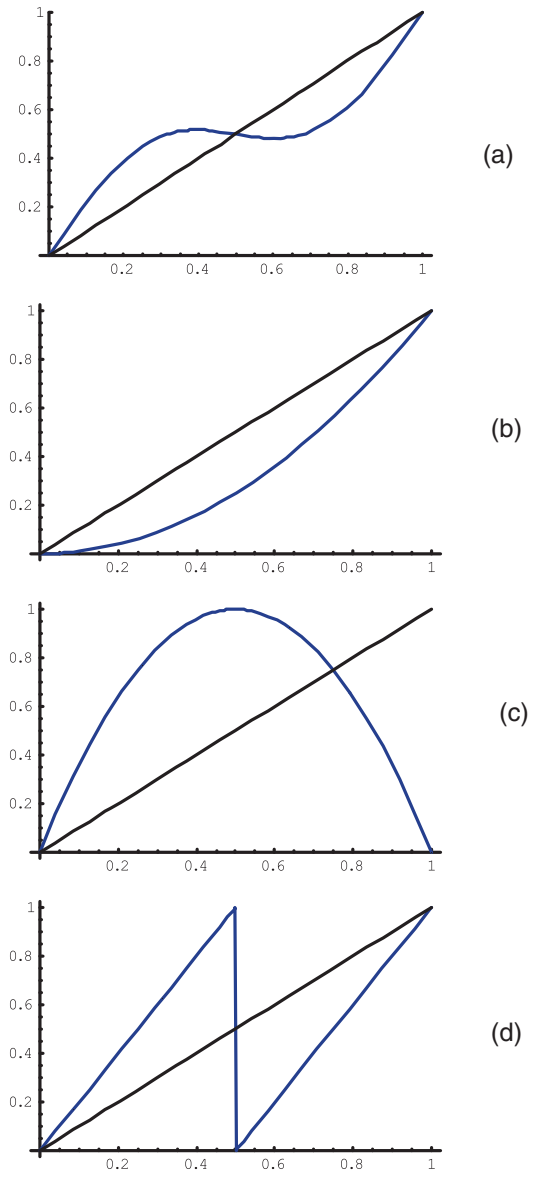


Figure 1.1: Examples of graphs of maps $f : \mathbb{I} \to \mathbb{I}$. Note that for (a), (b) orbits exhibit predictable behaviour, whereas for (c) and (d), a typical orbital behaviour is not apparent.

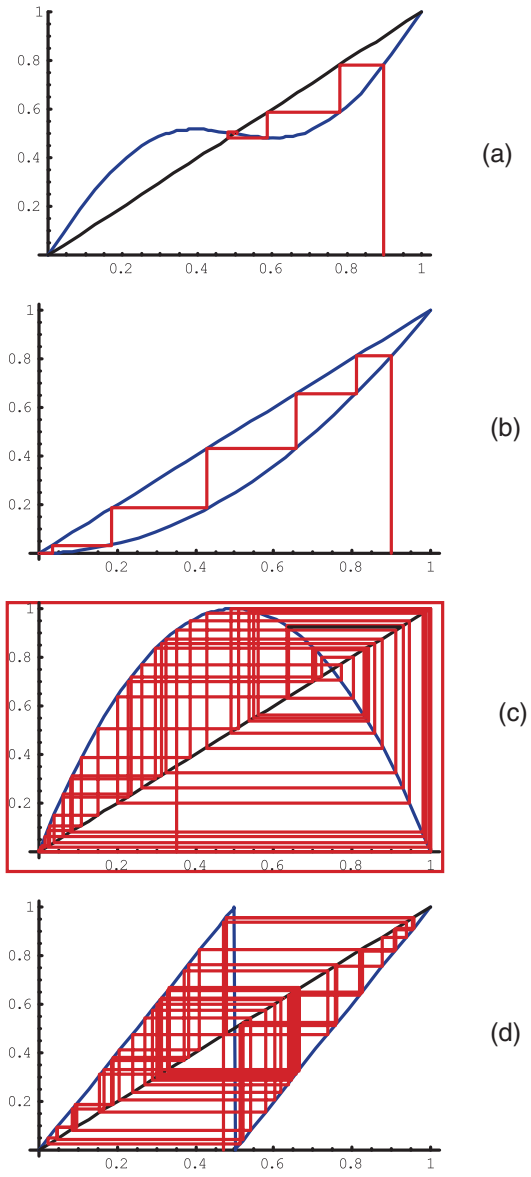


Figure 1.2: Orbit webs for the functions in Fig. 1.1 . Note the lack of any pattern in the orbit for (c) and (d). By contrast, orbit webs for functions (a)and (b) have obvious regularity and would produce a highly constrained binary sequence output. The maps for (a), (b) have orbits with predictable behaviour, whereas for (c),(d) a typical orbital behaviour is not apparent.

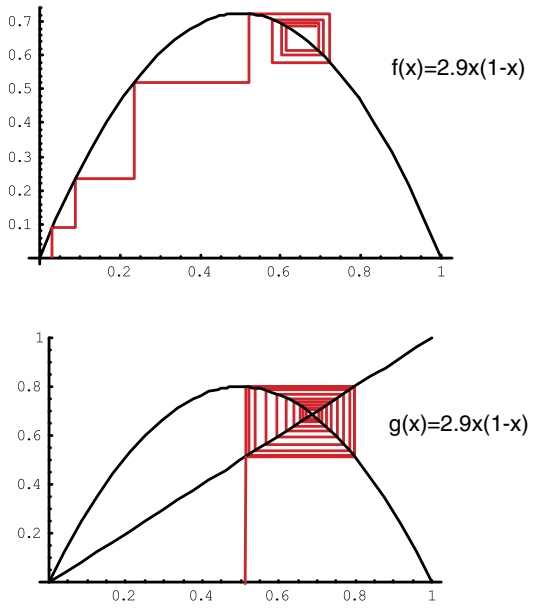


Figure 1.3: Various orbital behaviours in the neighbourhood of fixed point. One fixed is unstable, the other is stable.

Thus we have *asymptotic* stability for the fixed point $x^*$ when $|f'(x^*)| < 1$ and instability when $|f'(x^*)| > 1$.

*Periodic recurrence* is a generalization of the fixed point. A point $x = x_0$ is a *periodic point* of $f$ if $f^q(x_0) = x_0$ for some $q > 0$. The minimum such positive $q$ is said to be the *period* of the orbit which consists of the finite set $x_0, x_1, \ldots, x_{q-1}$ and which is then repeated infinitely since $x_q = x_0, x_{2q} = x_0$ etc. If $q = 1$ the periodic orbit is a fixed point, and if $q > 1$ the periodic orbit is non-trivial. The fixed point stability result extends to a $q$-periodic point $x^*$ by considering its behaviour as a *fixed* point of the map $f^q$. Thus the $q$-period periodic orbit $\{x_0, \ldots, x_{q-1}\}$ of $f$ is asymptotically stable if $|(f^q)'(x_0)| < 1$ and unstable for $|(f^q)'(x_0)| > 1$. The apparent dependence of stability on just $x_0$ and no other points of the periodic orbit is illusory as the derivative at $x = x_0$ that determines stability is given by

$$(f^n)'(x_0) = \prod_{i=0}^{q-1} f'(x_i), \tag{1.3}$$

and so $(f^n)'(x_i)$ is the same for all points $x_i$, $i = 0, \ldots q-1$ of the periodic orbit. It is possible for a map $f$ to become *eventually periodic*. An orbit with initial point $x_0$ can satisfy $f^q(x_k) = x_k$ for iterates $k > k_0$ only, for some fixed positive integer $k_0$. In this case, the orbit through $x_0$ is said to be *forward periodic*. Note that if the map $f : \mathbb{I} \to \mathbb{I}$ has an inverse map $g : \mathbb{I} \to \mathbb{I}$, then a forward periodic orbit of period $q$ is immediately periodic, i.e. $f^q(x_0) = x_0$. This follows from $f^q(x_k) = x_k$

by applying the map $f^{-k}$ to both sides.

The qualitative approach, which stems from a discussion of the properties described above has led to the discovery of the key ingredients of dynamical chaos. When allied with the great power of modern digital computers, these features can be easily displayed for systems and maps which have a simple analytical form. First, we consider some simple maps for which the dynamical complexity is relatively easy to uncover and describe.

## 1.3 Equivalence of maps

We can introduce an *equivalence* between maps which respects orbital behaviour. Let $\phi : \mathbb{I} \to \mathbb{I}$ be a homeomorphism, a map which is both bijective and bicontinuous. Suppose that we have two maps of the interval $f, g : \mathbb{I} \to \mathbb{I}$ such that the following *conjugacy* holds

$$g\phi(x) = \phi f(x)$$

for all $x \in \mathbb{I}$. We can deduce from the conjugacy that there is an equivalence of orbit structure for the maps $f$ and $g$. For any initial point $x_0 \in \mathbb{I}$, the $f$-orbit $\{f^n(x_0)\}$ and the $g$-orbit $\{g^n(y_0)\}$ with $y_0 = \phi(x_0)$ are in $1-1$ correspondence by the map $\phi$ where $\phi(f^n(x_0)) = g^n(y_0)$. Moreover, let $x_0$ be a periodic point of $f$ of minimum period $q$, i.e. $f^q(x_0) = x_0$ and $f^k(x_0) \neq x_0$ for $k < q$. Let $x_k = f^k(x_0)$, $k \in \mathbb{Z}^+$, then $\{x_0, x_1, \ldots x_{q-1}\}$ is the periodic orbit. Let $y_k = \phi(x_k)$. Then $\{y_0, y_1, \ldots y_{q-1}\}$ is a $q$-periodic orbit of the map $g$. Observe that the conjugacy gives $g^k\phi(x) = \phi f^k(x)$, $k \in \mathbb{Z}^+$. Thus

$$g^q(y_0) = g^q(\phi(x_0)) = \phi f^q(x_0) = \phi(x_0) = y_0,$$

and

$$g^k(y_0) = g^k(\phi(x_0)) = \phi f^k(x_0) \neq \phi(x_0) = y_0$$

using $\phi$ is injective, and $f^k(x_0) \neq x_0$. It follows that $y_0$ is a period-$q$ periodic point of $g$. Thus $\phi$ maps periodic orbits of $f$ to those of $\phi$, and, in particular, fixed points of $f$ to those of $g$. It can be similarly shown that aperiodic (i.e. non-periodic) orbits of $f$ are mapped to the aperiodic orbits of $g$. Eventually periodic orbits of $f$ and $g$ are also in $1-1$ correspondence. The bi-continuity of $\phi$ allows limiting structures of orbits to be associated. For example, the limiting set of an orbit of $f$ $L_f(x_0) = \lim_{n\to\infty} f^i(x_0)$, satisfies $\phi(L_f(x_0)) = L_g(y_0)$, where $y_0 = f(x_0)$. Limiting sets are sent to limiting sets.

## 1.4 Piece-wise linear maps

We can see that a linear map $f(x) = \alpha x$ with $\alpha \in \mathbb{R}$ has trivial dynamical behaviour. The map has a fixed point at the origin and orbital points either move away from the origin, or towards it,

depending on whether $|\alpha| > 1$ or $|\alpha| < 1$ respectively. Orbital diversity can be introduced with nonlinearity, see Figs 1.1 and 1.2.

### 1.4.1 The doubling map

The simplest nonlinear map of the interval can be constructed by using *two* linear components. It can be expressed in the form

$$D(x) = \begin{cases} 2x, & 0 \le x < 1/2 \\ 2x - 1, & 1/2 \le x < 11 \end{cases}, \tag{1.4}$$

or equivalently,

$$D(x) = 2x \pmod 1. \tag{1.5}$$

If we see the map $D$ as an iteration on $I' = [0, 1)$ defined by

$$x_n = 2x_{n-1} \pmod 1. \tag{1.6}$$

It is not difficult to 'solve' this equation and deduce that the $n$-th iterate $x_n = D^n(x_0)$ of $x_0 \in I'$ is simply given by

$$x_n = 2^n x_0 \pmod 1. \tag{1.7}$$

It is soon apparent that the solution is no more illuminating than the defining equation of $D$ simply because it is not at all clear how the exponential doubling interacts with the process of reducing mod 1.

The temptation at this point is to resort to the computer for more help and intuition. Unfortunately, we have only a finite number, say $m$, of binary places stored in the machine for each real number we wish to represent in $[0, 1)$ and we loose information at the rate of 1-binary place per iteration since, as we shall see, the map effectively shifts the binary expansion by one binary place and deletes the integer part. Thus if the computer fills out the number to $m$ places after each iteration in a controlled way by adding 0 in the $m$-th place, we have zero after $m$-iterations. If the $m$-th place is filled randomly, then after $m$ iterations we have a random number generator for binary $m$ digit integers. Clearly, the computer is not particularly useful here because of the exponential loss of information. A crucial feature of this map is the way in which orbits move apart. More precisely, the map offers *sensitive dependence on initial conditions* (Guckenheimer (1979), Devaney (1986)). Given any two distinct points of $x, x'$ of $I'$, their orbits initially diverge exponentially in the sense that $dist(D^n(x), D^n(x')) = 2^n dist(x, x')$ subject, of course, to the global constraint here that no two points can ever be more than distance one apart on $I'$. Thus, it is only locally that orbits are diverging exponentially.

**Coding and symbolic dynamics**

To understand the essential variety of the orbits available we return to the binary output map which reveals the nature of the dynamics and why such maps are appropriate for modelling digital sequence behaviour.

Any real number $x_0 \in I'$ can be written in the *binary form*

$$x_0 = \sum_{n=1}^{\infty} \frac{b_n}{2^n}, \tag{1.8}$$

where $b_n = 0$ or 1. Thus formally, we can represent each point of $I'$ as sequence $\sigma = \{b_n\}_{n=1}^{\infty}$. Let $\mathcal{S}$ denote the set of all such binary sequences. Now we note that

$$\begin{aligned} D(x_0) &= D\left(\sum_{n=1}^{\infty} \frac{b_n}{2^n}\right) \\ &= 2\sum_{n=1}^{\infty} \frac{b_n}{2^n} \pmod 1 \\ &= b_1 + \sum_{n=2}^{\infty} 2\frac{b_n}{2^n} \pmod 1 \\ &= \sum_{n=1}^{\infty} \frac{b_{n+1}}{2^n} \pmod 1 \end{aligned} \tag{1.9}$$

since $b_1$ is an integer. Thus formally we have a conjugacy

$$D\phi = \phi\alpha, \tag{1.10}$$

where

$$\phi(\{b_i\}_1^{\infty}) = \sum_{1}^{\infty} \frac{b_i}{2^i}. \tag{1.11}$$

Relative to this new formal representation of points in $I'$ as a binary sequence, the map $D$ takes the form of a *shift* $\alpha$ on binary sequences:

$$\{b_1, b_2, \ldots, b_n, \ldots\} \longmapsto \{b_2, b_3, \ldots, b_{n-1}, \ldots\}. \tag{1.12}$$

The map $\alpha$ is defined precisely by

$$\alpha(\{b_n\}_{n=1}^{\infty}) = \{b_{n+1}\}_{n=1}^{\infty}. \tag{1.13}$$

This straightforward observation allows us to examine the periodic structure of the map $D$. We note that the period-$q$ periodic points of $\alpha$ in $\mathcal{S}$ are precisely those binary representations for $x_0$ that repeat after $q$-digits and no fewer. Thus a period-1 point of $\alpha$ is given by the repeating expansions

$$\sigma_1 = \{00000\ldots\} = \{\overline{0}\}.$$

Period-2 points are given by

$$\sigma_2 = \{010101\ldots\} = \{\overline{01}\}, \tag{1.14}$$

and

$$\sigma_3 = \{101010\ldots\} = \{\overline{10}\}. \tag{1.15}$$

Clearly the sequence $\sigma_1$ is the binary representation of $x = 0$ and $D(0) = 0$. The sequence $\sigma_2$ gives the point $x = 1/4 + 1/16 + 1/64 + \ldots = 1/3$ and $\sigma_3$ gives the point $x = 2/3$. Note either by using $\alpha$ on the two symbols $\sigma_2$ and $\sigma_3$ or $D$ on the corresponding real values $1/3, 2/3$ we have period-2 orbits. Specifically,

$$\alpha(\sigma_2) = \sigma_3, \quad \alpha(\sigma_3) = \sigma_2 \tag{1.16}$$

and the corresponding

$$D(1/3) = 2/3, \quad D(2/3) = 1/3, \tag{1.17}$$

respectively. Note that the orbit web for a periodic orbit such as this closes up after 2 iterations. Points which have orbits which are *eventually* period one or two can be obtained by delaying the introduction of the recurrences given in the above symbolic sequences, e.g. the orbit $\sigma = 1101010\overline{0}$ is eventually a fixed point since $\alpha^6(\sigma) = \overline{0}$ and remains at $x = 0$. We can see immediately that periodic points of all orders can be constructed for $\alpha$ in this way and therefore there are corresponding periodic orbits for the map $D$.

A key observation on the type of orbits available from such a map comes from noting that if $\{b_n\}_{n=1}^{\infty}$ is the binary sequence arising from the binary representation of the point $x$ then $x \leq 0.5$ if $b_1 = 0$ and $x \geq 0.5$ if $b_1 = 1$. Given that iteration of $D$ corresponds to shifting the symbols of the binary sequence, we see that it provides, *at a glance*, the movement of the itinerary of the orbit through the regions '0' representing the interval $I_0 = [0, 0.5)$ and '1' representing $I_1 = [0.5, 1)$.
*Remark* This statement is only strictly true if we are careful about the ambiguity of binary representation. Note that $0.5 = 0.10000\ldots = 0.011111\ldots$. In fact, for every real number whose infinite binary expansion finishes in consecutive zeroes can also be expressed using an infinite sequence of ones. If we always choose zeroes for these ambiguous cases (the dyadic numbers) then the itinerary described above is accurate. So we see that these piecewise linear maps can give rise to all possible binary sequences and so this demonstrates the flexibility of the maps to create all experimental cases of ON-OFF binary data.

By investigating the graph of the map $D$ we can see that sub-intervals of $\mathbb{I}$ can be located which give rise to the various sequences of binary data. For example, it is easy to check that for the doubling map, we have the following correspondences for one and two symbols:

$$\begin{array}{cc} [0, 0.5) - \text{`}0\text{'}; & [0.5, 1) - \text{`}1\text{'}; \\ [0, 0.25) - \text{`}00\text{'}; & [0.25, 0.5) - \text{`}01\text{'}; \\ [0.5, 0.75) - \text{`}10\text{'}; & [0.75, 1.0) - \text{`}11\text{'}; \end{array} \tag{1.18}$$

There are eight symbol sequences of length 3 and each sequence arises from a unique closed-open interval of length 1/8 etc. . For example,"000" for any initial point $x_0 \in [0, 1/8)$. Obviously, an infinite binary sequence arises from a unique real value as the defining interval lengths reduce to zero. Carrying this through all the finite sequences gives the symbolic encoding of the map $D$.

### 1.4.2 Other piecewise linear maps

Variations on the doubling map $D$ are the *tent* map $T : \mathbb{I} \to \mathbb{I}$:

$$T(x) = \begin{cases} 2x, & 0 \leq x \leq \frac{1}{2}, \\ 2 - 2x, & 1/2 \leq x \leq 1. \end{cases}$$

and the $m$-fold *sawtooth* map $S_m : \mathbb{I} \to \mathbb{I}$:

$$S_m(x) = mx \pmod 1.$$

The map names reflect the appearance of their graphs. Note that the doubling map $D$ is also given by the special sawtooth map $S_2$. The tent map has a symbolic coding on 2-symbols, and the sawtooth requires m-symbols, one for each of the intervals $[\frac{k}{m}, \frac{k+1}{m}]$, $k = 0, 1, \ldots, m-1$.

### 1.4.3 Chaos in maps

All of the above maps iterate to give *chaotic* behaviour:

1. initial states move apart exponentially and are said to have *sensitive dependence on initial conditions*;

2. the map has dense orbits, [Devaney (1986)], that is, the orbit passes arbitrarily close to every point of the interval;

3. the set of periodic points of the map are dense in the interval.

All of the maps with two (or more) continuous segments can be shown to exhibit the flexible orbital behaviour of the chaotic doubling map. The doubling, tent and quadratic maps cannot be distinguished *topologically* because symbolically, they are indistinguishable. An, apparently, similar type of map $g(x) = 3x \pmod 1$ on $\mathbb{I}$ is, in fact, different, as it requires *three*, rather than two, symbols to describe itineraries with '$0' = [0, 1/3)$, '$1' = [1/3, 2/3)$, '$2' = [2/3, 1)$. The map $g$ differs from the doubling map in its periodic point structure. For example, $g$ has the following period-2 periodic orbits -

$$\{\{\overline{01}\}, \{\overline{10}\}\}, \tag{1.19}$$

$$\{\{\overline{02}\}, \{\overline{20}\}\}, \tag{1.20}$$

$$\{\{\overline{12}\},\{\overline{21}\}\}, \tag{1.21}$$

whereas $D$ has just one period-2 periodic orbit, namely $\{\{\overline{01}\ldots\},\{\overline{10}\ldots\}\}$. This observation shows that the maps $S_3$ with $D$ are not conjugate as there is a 1-1 correspondence of period-$q$ orbits for such maps. Similar considerations will show that $S_m$ and $S_n$ are not conjugate for $m \neq n$.

The symbolic coding allows us to check conditions (ii) and (iii). The sensitive dependence on initial conditions shows up directly from the nature of the map $D$ - the images of two points distance $d$ apart are $2d$ apart when $d$ is sufficiently small.

The existence of dense orbits follows from the construction of a symbol sequence with all possible symbolic words. This can be done by listing in sequence all possible symbol sequences of all possible lengths.

The density of periodic orbits in $\mathbb{I}$ can be shown by observing that any point $x$ with symbol sequence $\{b_i\}_{i=1}^{\infty}$ can be approximated increasingly well by symbolic sequences which are periodic with longer and longer periods.

## 1.5 Invariant densities and measures

Let us consider the output from two maps of the same type from the previous section. The graphs of both maps (a) $D(x) = 2x \pmod 1$, and (b)

$$f(x) = \begin{cases} x + 2x^2, & 0 \leq x < 0.5, \\ 2x - 1, & 0.5 \leq x \leq 1 \end{cases}, \tag{1.22}$$

consist of two curves with a single discontinuity at $x = 0.5$.

How can the behaviour illustated in Fig. 1.4 be generated or predicted by changing the the characteristics of the map? To answer this we have to consider how orbits distribute themselves both temporally and spatially and whether this can be characterized for almost all orbits. For this we need to develop the idea of *invariant densities* and the related concept of *invariant measure* for a map.

### 1.5.1 Orbital densities

We consider the distributions of numbers generated by orbits of (a) the doubling map, $D$, and (b), the quadratic map, $Q$. The map is iterated for $M = 10^6$ times for the doubling map, and $M = 10^5$ for the quadratic map. The unit interval is divided into $N$ small equal length intervals where $N = 50$. We see an even distribution of visits to the intervals. There is a 'smoothing' of the distribution as the number of iterations $M$ is increased.

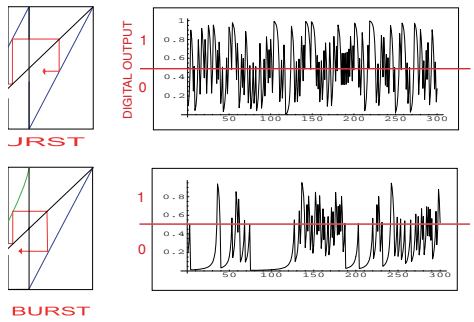


Figure 1.4: Orbits for random initial conditions for maps (a) $D$, and (b) $f$ in eqn (1.23). For each map we have the real orbital data and the corresponding integer orbital data using the output map $s$. There are clear differences: the digital crossover from '0' to '1' is much more regular for map (a) and the lengths of spells of '0's are much longer for map (b). This is caused by the tangency of the $\mathrm{gr}(f)$ with the line $y = x$ at the origin.

### 1.5.2 Perron-Frobenius Theorem

It can be shown theoretically that the apparent smoothing of the distribution in Fig. 1.5 (a) to a constant function actually occurs. Consider a probability distribution $\rho_0$ on the interval $\mathbb{I}$ which describes the distribution of a large ensemble of initial conditions for the map $D$. Let the evolution of the ensemble $\rho_0$ after $n$ iterations of $f$ be given by the probability distribution $\rho_n$. The effect of one iteration on $\rho_n$ is

$$\rho_{n+1}(x) = \int_0^1 \delta(x - f(z))\rho_n(z)\, dz. \tag{1.23}$$

A justification for this result can best be seen by thinking of the distribution as arising from an orbit count. Let us consider the orbit $\{x_n\}_{n=0}^{\infty}$. Then the probability of orbital values taking the value $y$ is

$$\rho_0(y) = \lim_{N\to\infty} \frac{1}{N} \sum_{i=1}^{N} \delta(y - x_i), \tag{1.24}$$

where the *delta* function $\delta$ satisfies

$$\delta(x) = \begin{cases} 1 & x = 0, \\ 0 & \text{otherwise}, \end{cases} \tag{1.25}$$

and

$$\int_{-\infty}^{\infty} \delta(x - x_0) f(x) dx = f(x_0) \tag{1.26}$$

The integral $\int \delta(y - f(x))\delta(x - x_i)dx$ takes the value 1 when both $y = f(x)$ and $x = x_i$, and zero otherwise. Thus

$$\int \delta(y - f(x))\delta(x - x_i)dx = \delta(y - x_{i+1}). \tag{1.27}$$

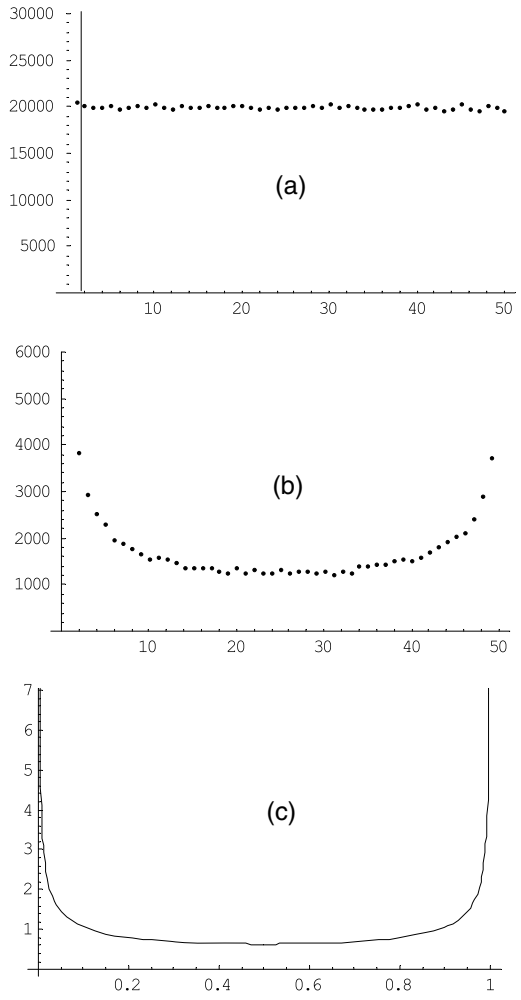


Figure 1.5: The distribution of orbital points for (a) the doubling map, $D(x)$ and (b), the quadratic map, $Q(x) = 4x(1-x)$.
These are *natural* distributions that occur for almost all initial conditions. The natural distribution approximated above is given by the function

$$\rho(x) = \frac{1}{\pi\sqrt{(}x - x^2).}$$

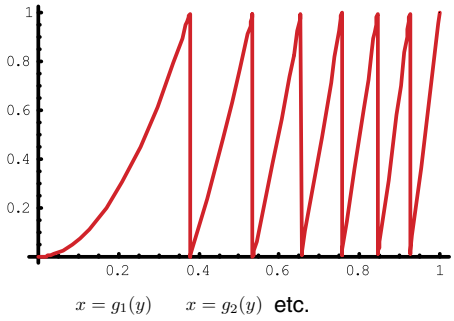


Figure 1.6: The function $f(x) = 6x^2 \bmod 1$ splits into several components homeomorhisms $f_1$,$f_2$,...,$f_6$ which are surjective onto the interval. Each component function $x = f_i(y)$ has an inverse $x = g_i(y)$.

The distribution of points $\rho_0$ evolves to the distribution $\rho_1$ where (cf. 1.24)

$$\rho_1(y) = \lim_{N\to\infty} \frac{1}{N} \sum_{i=1}^{N} \delta(y - x_{i+1}), \tag{1.28}$$

since the set of points $\{x_i\}_{i=1}^{\infty}$ evolves to $\{x_{i+1}\}_{i=1}^{\infty}$, and using (1.27), we obtain

$$\begin{aligned} \rho_1(y) &= \lim_{N\to\infty} \frac{1}{N} \sum_{i=1}^{N} \delta(y - x_{i+1}) \\ &= \lim_{N\to\infty} \frac{1}{N} \sum_{i=1}^{N} \delta(y - f(x))\delta(x - x_i) \\ &= \int \delta(y - f(x)) \lim_{N\to\infty} \frac{1}{N} \sum_{i=1}^{N} \delta(x - x_i)dx \\ &= \int \delta(y - f(x))\rho_0(x)dx \end{aligned} \tag{1.29}$$

If the functional relation $\rho_0 \to \rho_1$ is written as $\rho_1 = \mathcal{P}(\rho_0)$ the functional operator $\mathcal{P}$ is known as the *Perron-Frobenius* operator. Exploiting the definition of the $\delta$ function it can be written in different forms.

Suppose that the graph $f$ is composed from several continuous components

$$f_1, f_2, \ldots, f_n,$$

each of which has function inverses

$$g_1, g_2, \ldots g_n.$$

Then $f^{-1}(y) = \{g_1(y), \ldots, g_n(y)\}$ and we have

$$\rho_1(y) = \int_{x\in f^{-1}(y)} \rho_0(x)dx = \sum_{i=1}^{n} \rho_0(g_i(y))|g_i'(y)|, \tag{1.30}$$

as when the functions $g_i$ are differentiable, $dx = g_i'(y)dy$.

We can use the fact that $f$ and $g_i$ are inverse functions to re-write the Perron-Frobenius equation. The equivalence $f(x)g(y) = 1$ when differentiated gives $f'(x)g_i'(y) \equiv 1$, and so

$$\rho_1(y) = \sum_{i=1}^{n} \frac{\rho_0(x_i)}{|f'(x_i)|}, \tag{1.31}$$

if $f^{-1}(y) = \{x_1, x_2, \ldots, x_n\}$, a finite set.

If the probability distribution $\rho_0$ does not change with time under iteration, it is referred to as an *invariant* density and it satisfies $\rho_0 = \rho_1 = \rho$, i.e.

$$\rho(y) = \int_0^1 \delta(y - f(z))\rho(z)\, dz, \tag{1.32}$$

is called an *invariant density* of the map, and Eq. (1.32) is known as the Perron-Frobenius equation. There are many invariant densities. For example, let

$$\{x_0, x_1, \ldots, x_{q-1}\}$$

be a period-$q$ periodic orbit. Then

$$\rho(x) = \begin{cases} 1/q & x = x_i \\ 0 & \text{otherwise} \end{cases} \tag{1.33}$$

is an invariant probability density. However, the latter density is *singular* in the sense that it is zero almost everywhere in the interval. For the doubling map, orbital calculations can result in information on measures. The invariant measures for the doubling map split into three types. The discrete measures arise for (a) periodic and eventually periodic points, (b) typical, or *normal* irrational points,[Hardy(1979)], and finally (c), atypical irrational points. For the doubling map the *natural* invariant measure arises from the orbital distributions associated with normal initial points. The normal points form a set of measure one in $\mathbb{I}$. It should be noted that periodic points which form the singular measures are also dense in $\mathbb{I}$ but more importantly, they have zero measure. Essentially, all finite patterns of digits are equally likely to occur in its binary expansion. Thus normal numbers must be irrational as rational numbers have cyclic binary expansions and therefore a restricted set of digital patterns. One would expect that the points of an orbit through such a normal number would therefore spread evenly over the interval and that the natural invariant measure $\rho$ for the doubling map $f$ is uniform, i.e. $\rho(x) \equiv 1$. We can check that it satisfies the Perron-Frobenius equation. It is easy to construct initial irrational values, which therefore do not give rise to periodic orbits, which will not give a uniform distribution on the interval $\mathbb{I}$. For example, the orbit of the point $x_0$ represented symbolically by

$$x_0 = 01001000100001000001, \ldots$$

clearly spends most of its time in the '0′ region when iterated by $D$. In fact, asymptotically, the proportion of its time spent in the '0′ region tends to 1.

The invariant measure associated with this orbit is actually singular at $x = 0$, i.e a *delta* function at zero, $\delta(x)$, so that $\int_0^1 \delta(x)dx = 1$.

### 1.5.3 Invariant measures

Given an invariant density $\rho$ for $f : X \to X$, we can consider an associated invariant *measure* $\mu$ where

$$\mu(S) = \int_S d\rho = \int_S \rho(x)dx$$

on subsets $S$ of the space $X$.

The measure associated with the map $f$ has invariance properties. Consider

$$\mu(f^{-1}(S)) = \int_{f^{-1}(S)} \rho(x)dx.$$

The change of variable $y = f(x)$ implies $y \in S \iff x \in f^{-1}(S)$. The invariant density $\rho$ implies $\rho(y)dy = \rho(x)dx$ and so we deduce

$$\mu(f^{-1}(S)) = \int_{f^{-1}(S)} \rho(x)dx = \int_S \rho(y)dy$$

and the measure invariance for $f$ can be written as

$$\mu(f^{-1}(S)) = \mu(S).$$

Thus the measure is preserved for inverse images. This is true regardless of whether $f$ has a map inverse. For example with doubling map $D$ or the tent map $T$, the inverse image of a interval of length $d$ is the union of two intervals each of length $d/2$. The property does not extend to forward images, unless $f$ is bijective in which case forward images of $f$ are inverse images of $f^{-1}$.

### 1.5.4 Invariant densities for simple maps

#### The doubling map

Let $y \in \mathbb{I}$, then $D^{-1}(y) = \{y/2, (1+y)/2\}$ for the doubling map $D$ and $D'(y/2) = D'((1+y)/2) = 2$. Then

$$\rho(y) = \frac{\rho(y/2)}{2} + \frac{\rho((1+y)/2)}{2} \tag{1.34}$$

is satisfied by the constant map $\rho = 1$. The argument can be easily extended to the sawtooth map $S_m$ for $m > 2$.

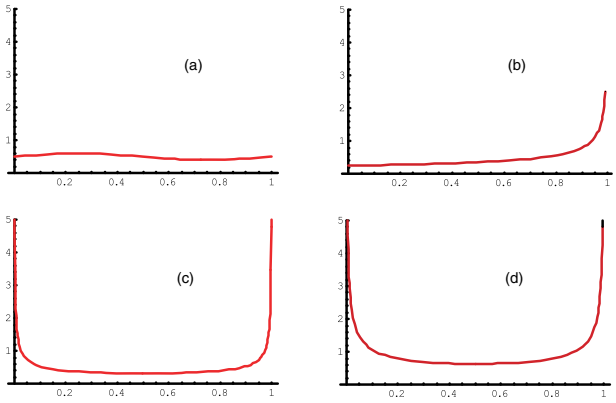


Figure 1.7: For the quadratic map $Q(x) = 4x(1-x)$, the initial density is (a) $\rho_0(y) = 0.5 + 0.1\sin(2\pi y)$ (Remark: an arbitrary choice); and various iterates of $\rho_0$ by the Perron-Frobenius operator $P_Q$ to (b) $\mathcal{P}_Q^1(\rho_0)$, (c) $\mathcal{P}_Q^8(\rho_0)$ which converge in (d) to the natural invariant density $\rho_Q$ of the map $Q$.

### The tent map

The tent map $T$ is closely associated with the doubling map and is also a piece-wise linear version of the quadratic map defined by $T(x) = 2x$ for $0 \leq x < 0.5$ and $T(x) = 2 - 2x$ for $0.5 \leq x < 1$. That $\rho(x) \equiv 1$ is also an invariant density for $T$ is not difficult to show. Consider a measurable set $S \subseteq \mathbb{I}$. Then $T^{-1}(S) = S^{(1)} \cup S^{(2)}$ where $S^{(1)} = \{x/2 | x \in S\}$ and $S^{(2)} = \{(2-x)/2 | x \in S\}$. Given $\mu(S^{(1)}) = \mu(S^{(2)}) = \mu(S)/2$, for the density $\rho$, we have that it is invariant.

### The quadratic map

We consider the quadratic map

$$Q(x) = 4x(1-x)$$

.

We show that

$$\rho_Q(y) = \frac{1}{\pi}\frac{1}{\sqrt{y(1-y)}}$$

is an invariant density for the map $Q$. The pre-images of the point $y$ by the map $Q$ are $x = (1 \pm \sqrt{(1-y)})/2$ and $f'(x) = 4 - 8x|_x = \mp 4\sqrt{(1-y)}$. The function

$$\rho_Q(y) = \frac{1}{\pi}\frac{1}{\sqrt{y(1-y)}}$$

satisfies the identity

(1.35)

$$\rho_Q(y) = \frac{\rho_Q((1+\sqrt{(}1-y))/2)}{|-4\sqrt{(}1-y)|} \tag{1.36}$$

$$+ \frac{\rho_Q((1-\sqrt{(}1-y))/2)}{|4\sqrt{(}1-y)|}, \tag{1.37}$$

$$\tag{1.38}$$

can be checked to confirm the Perron-Frobenius equation for the density $\rho_Q$.

**Densities induced by conjugacy**

An alternative approach to finding the invariant density for the map $Q$ is to consider the conjugacy which relates it to the tent map $T$ and transfer the invariant density from $T$ to $Q$ via the conjugacy.

Consider the map $\phi : \mathbb{I} \to \mathbb{I}$ where

$$\phi(x) = \sin^2(\frac{\pi x}{2}).$$

Observe that for $x \in [0, 0.5]$

$$\begin{aligned} Q\phi(x) &= 4\sin^2(\frac{\pi x}{2})(1-\sin^2(\frac{\pi x}{2})) \\ &= \sin^2(2\frac{\pi x}{2}) \\ &= \phi(2x) = \phi(T(x)). \end{aligned} \tag{1.39}$$

For the interval $x \in [0.5, 1]$,

$$\begin{aligned} Q\phi(x) &= 4\sin^2(\frac{\pi x}{2})(1-\sin^2(\frac{\pi x}{2})) \\ &= \sin^2(2\frac{\pi x}{2}) \\ &= \sin^2(2\frac{\pi(1-x)}{2}) \\ &= \phi(2-2x) \\ &= \phi T(x). \end{aligned} \tag{1.40}$$

Thus $\phi$ provides a conjugacy between the maps $T$ and $Q$ with $Q\phi(x) \equiv \phi T(x)$. The conjugacy $y = \sin^2\left(\frac{\pi x}{2}\right)$ is a differentiable change of coordinates and the natural measure $\rho_T(x) \equiv 1$ is transferred to the invariant measure $\rho_Q$ via the map $\phi(x) = \sin^2(\frac{\pi x}{2})$. Observe

$$\begin{aligned} \frac{d\phi(x)}{dx} &= 2\sin(\frac{\pi x}{2})\cos(\frac{\pi x}{2})\frac{\pi}{2} \\ &= \pi\sqrt{y}\sqrt{(}1-y). \end{aligned} \tag{1.41}$$

Therefore

$$\frac{dy}{\pi\sqrt{y(1-y)}} = 1.dx$$

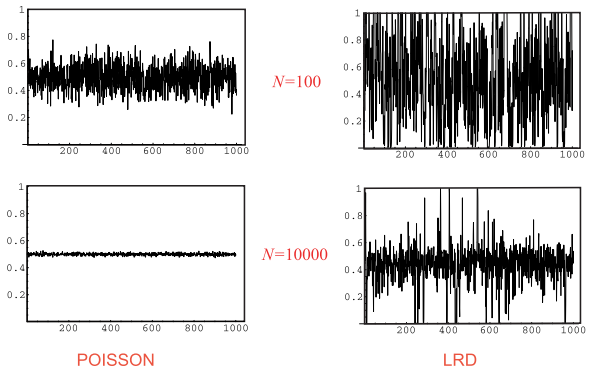


Figure 1.8: If a time series $X_i$, $i = 1 \ldots K$ is sampled with batch sizes of $N$, i.e $Y_j = \sum_{i=jN+1}^{(j+1)N-1} X_i$, then the variance of the sample $Y_j$ will decrease as $N$ is increased. The rate of the decrease depends on the nature of the time series $X_i$. Specifically, as batch size $N$ is increased, the doubling map has rapidly diminishing by comparison with a map that exhibits intermittency.

and so the density $\rho_T(x) = 1$ transfers to

$$\rho_Q(y) = \frac{1}{\pi\sqrt{y(1-y)}}.$$

## 1.6 Intermittency

The use of dynamical systems in the context of this exposition is to provide a method for giving statistically appropriate digital output from an iterative scheme. One aspect of digital output that is of interest if the nature of the auto-correlation decay of an output sequence or a family of sequences. In particular power-law decay of the auto-correlation is seen to have *memory* or *long-range dependence*, whereas exponential decay is seen to have no memory or *short-range dependence*. A necessary ingredient of the output in this situation is a slow decrease in the variance as the size of the batch averages are increased. We will return to this later. The method of achieving this is to ensure that orbits spend long periods in the 'ON' and 'OFF' regimes thus ensuring that averages of large batch size can still be either 0 or 1 and not the 0.5 arising form the doubling map. We achieve this by introducing *intermittency* into the iterative map $f$.

Intermittency is achieved by having segments of $gr(f)$ given by $y = f(x)$ arbitrarily close to the fixed point line $y = x$ map. In Fig. 1.8 we see two levels of behaviour from this point of view. In (a), the graph meets the line $y = x$ in a fixed point $x = x^*$. Iteration from $x_0$ then accumulates at $x^*$ and the iteration takes increasingly small steps. Note that such a scenario could produce an infinity of either consecutive zeroes or ones depending on the location of the point $x^*$. By comparison, a graph which is close to the line $y = x$ provides a region of small iterative steps. If the graph

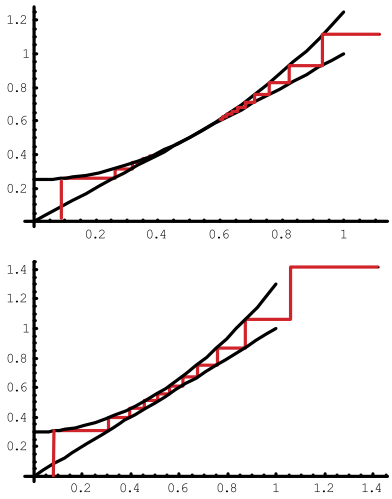


Figure 1.9: Different types of orbital behaviour for different locations of the graph of $f$ relative to the fixed point line $y = x$. Note that in (a), there are three types of orbit for an initial point $x_0$. There is (i) a fixed point orbit at $x_0 = x^*$, (ii) orbits that have $f^n(x_0) \to x^*$ as $n \to \infty$, and (iii) orbits that have $f^n(x_0) \to x^*$ as $n \to -\infty$

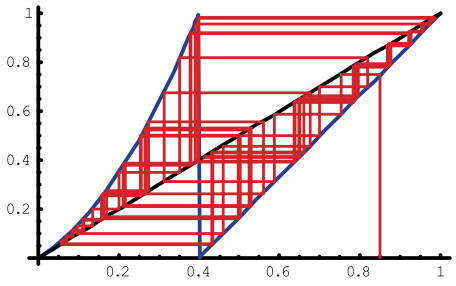


Figure 1.10: A piecewise continuous map $f : \mathbb{I} \to \mathbb{I}$ defined with intermittency at $x = 0$.

is relatively remote from the line $y = x$, i.e case (c), then large iterative steps occur. Excluding the extreme case (a), we say that (b) provides output with 'long memory' and (c) provides output with 'short memory'. To show more precisely how these geometrical cases provide differences in the binary output, we will consider a case of intermittency at the point $x = 0$.

Let $f : \mathbb{I} \to \mathbb{I}$ be defined by

$$f(x) = \begin{cases} x + (1-d)(\frac{x}{d})^m & 0 \leq x < d \\ \frac{x-d}{1-d} & d \leq x < 1. \end{cases} \tag{1.42}$$

and the output $s : \mathbb{I} \to \{0, 1\}$ with

$$s(x) = \begin{cases} 0 & 0 \leq x < \bar{d}, \\ 1 & \bar{d} \leq x \leq 1. \end{cases}$$

Fig. 1.11 has $d = 0.4$ and $m = 2$.

Note that it is not necessary to have $\bar{d} = d$. We choose $m > 1$ to ensure an intermittency effect. We are interested in the lengths of consecutive sequences of '0's in the binary output. If we consider the simpler piece-wise linear case of $g : \mathbb{I} \to \mathbb{I}$ with

$$g(x) = \begin{cases} \frac{x}{d} & 0 \leq x < d \\ \frac{x-d}{1-d} & d \leq x < 1. \end{cases}$$

The slope of the first branch of $g$ is $1/d$ and we can calculate immediately that a "zero" sequence will be of length $k$ if the initial point $x_0$ lies in the interval $[\bar{d}d^k, \bar{d}d^{k-1})$. Given that the natural invariant density of the map $g$ is $\rho(x) = 1$, we have that the probability of a string of consecutive zeroes of length k, given that $x_0$ is in $[0, \bar{d})$, is $P(k) = d^{-k}$ and the probability of a string of consecutive zeroes of at *least* length $k$ is $P_{\leq}(k) = d^{-(k+1)}$. Therefore, the probability of obtaining increasingly long strings of zeroes decays exponentially in the piece-wise linear case.

### 1.6.1 Closed form intermittency

We now return to the intermittent case. The simplest map exhibiting intermittency was given as $f : [0, d] \to [0, 1]$ where $f(x) = x + (1-d)(\frac{x}{d})^m$. However, somewhat surprisingly it is much easier to work with the map

$$\hat{f}(x) = \frac{x}{(1 - \hat{d}x^{m-1})^{\frac{1}{m-1}}}.$$

First of all, the map $\hat{f}$ belongs to the same family as $f$ since an expansion in series gives

$$\hat{f}(x) = x + \frac{\hat{d}}{m-1}x^m + \mathrm{O}(x^{m+1}),$$

and therefore has the same leading degree of intermittency. However, the map $\hat{f}$ has the striking property of being algebraically closed under dynamical iteration. It can be shown

$$\hat{f}^k(x) = \frac{x}{(1 - k\hat{d}x^{m-1})^{\frac{1}{m-1}}},$$

for $k = 0, 1, 2, \ldots$ . This formula extends sensibly to real values of $k$ given the monotonic nature of the function.

*Remark*Forcing the coefficients of $x^m$ for $f$ and $\hat{f}$ to be the same is not the appropriate indentification for the two maps as $\hat{f}$ has infinite asymptotic behaviour when $(1 - \hat{d}x^{m-1}) = 0$. The best approximation is obtained by requiring $\hat{f}(d) = 1$, which implies $\hat{d} = (1 - d^{m-1})/d^{m-1}$.

Suppose that we are now interested in the behaviour of escape from the region $[0, \bar{d}]$ by iteration of the map $\hat{f}$. The point $x = x(k)$ which escapes to infinity in exactly $k$ iterations, i.e. $\bar{d} = f^k(x(k))$, escapes. Solving for $x(k)$ we have

$$x(k) = \frac{\bar{d}}{(1 + k\hat{d}\bar{d}^{m-1})^{\frac{1}{m-1}}}.$$

As $k \to \infty$, we have

$$x(k) \sim K(\hat{d}, \bar{d})k^{\frac{-1}{m-1}}.$$

By solving the above equation for $k$, we see that the number of iterations $k$ to escape is

$$k(x) = \frac{1}{\hat{d}}\left(\frac{1}{x^{(m-1)}} - \frac{1}{\bar{d}^{(m-1)}}\right) \tag{1.43}$$

and so we obtain

$$k \sim \frac{1}{\hat{d}}x^{-(m-1)}.$$

Strictly, we should take $k$ to obtain the integer solution for the number of iterates to escape since $k \in \mathbb{R}$. If $f$ also has intermittency at $x = 1$, a similar integer function can be found which gives the number of consecutive ones for an initial condition $x_0 > d$. These equations are not available for the simpler functional form $f$.

### 1.6.2 Intermittency for non-differentiable maps

It is possible to consider piecewise linear maps which can emulate the intermittency properties of its smooth counterparts. We use the monotonic decreasing sequence $z_0 = 1$ $z_i = 0.5i^{-a}$, $a > 1$ and $i \geq 1$ to create the sequence of nodal points $\{(z_{i+1}, z_i)\}_1^\infty \subseteq \mathbb{R} \times \mathbb{R}$, see Fig. 1.11. When the points are consecutively joined, we obtain a graph of a monotonic function $p$ on the interval $[0, 0.5]$ with values in the range $[0, 1]$.

Essentially, $p(z_{i+1}) = z_i$, $i = 0, 1, \ldots$ with linearity between these points. Contrasting with the continuous case, we have

$$f(x) = x + ax^m + \ldots$$

and so

$$\lim_{x \to 0} \frac{\ln(f'(x) - 1)}{\ln(x)} = m - 1. \tag{1.44}$$

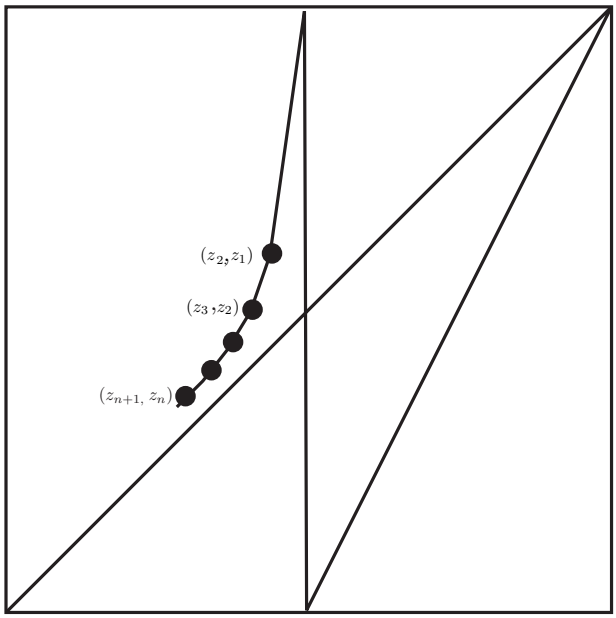


Figure 1.11: Piecewise linear map segments constructed from a sequence $z_i$ with vertex points $(z_2, z_1)$, $(z_3, z_2)$, $(z_4, z_3)$,... $(z_{n+1}, z_n)$,...

We now consider the corresponding calculation for the map $p$. We have $z_i = i^{-a}$ and so $\ln z_i = -a \ln i$. The piecewise linear segment on the interval $[z_{i+1}, z_i]$ has the slope

$$\mu_i = \frac{z_{i-1} - z_i}{z_i - z_{i+1}}.$$

Thus the corresponding calculation for $f$ in eqn.(1.41) when applied to $p$ yields

$$\begin{aligned} \lim_{i\to\infty} \frac{\ln(\mu_i - 1)}{\ln(z_i)} &= \lim_{i\to\infty} \frac{\ln(\frac{(i-1)^{-a} - 2i^{-a} + (i+1)^{-a}}{i^{-a} - (i+1)^{-a}})}{\ln(z_i)} \\ &= \lim_{i\to\infty} \frac{\ln(\frac{(a+1)}{i})}{-a \ln i} \\ &= \frac{1}{a}. \end{aligned} \tag{1.45}$$

Comparing the equations (1.44) and (1.45), we obtain

$$m = \frac{1+a}{a}. \tag{1.46}$$

The range $m \in [3/2, 2]$ for the smooth case is shown to be of importance in the next section. Note that it corresponds to the range $a \in [1, 2]$ for $p$ by equation (1.46).

**Invariant density for the a double intermittency map**

Let $p$ be defined as above relative to the sequence of points $z_i^L = 0.5i^{-a}$ for the interval [0.5],and $z_i^R = 1 - 0.5i^{-b}$ for the interval $[0.5, 1]$, with $a, b > 1$, see Fig. 1.10.

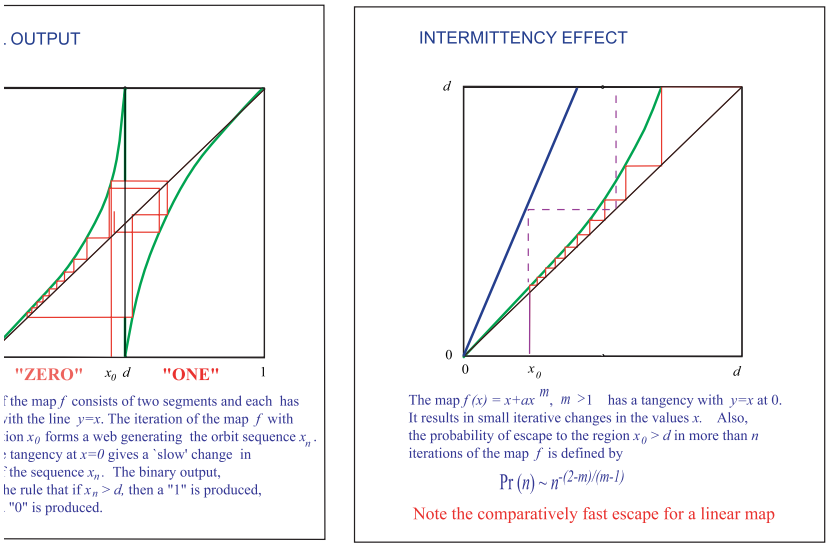


Figure 1.12: (a) The digital output from a map. (b) The effect of intermittency on the orbits near $x = 0$.

We look for an invariant density for $p$ which is piece-wise constant, and equal to $\rho_i^L$ on each of the intervals $L_i = [z_{i+1}^L, z_i^L]$ in $[0, 0.5]$ and equal to $\rho_i^R$ on each interval $R_i = [z_i^R, z_{i+1}^R]$ in $[0.5, 1]$. In Fig. 1.11, we see that the pre-images of a point in $x \in L_i$ are in $L_{i+1}$ and $R_1$. Similarly, the pre-images of a point $x \in R_i$ are in $R_{i+1}$ and $L_1$. Note points of $L_{i+1}, R_{i+1}$ map exclusively to $L_i, R_i$ respectively. By comparison $L_1$ maps by $p$ to the interval $[0.5, 1] = \cup_{i=1}^{\infty} R_i$, and $R_1$ maps to the interval $[0, 0.5] = \cup_{i=1}^{\infty} L_i$. Let $s_i^L, s_i^R$ be the slope of the graph of $p$ on the intervals $L_i, R_i$ respectively. Using this information in the *Perron-Frobenius* theorem, we have

$$\rho_i^L = \frac{\rho_{i+1}^L}{s_{i+1}^L} + \frac{\rho_1^R}{s_1^R}; \qquad \rho_i^R = \frac{\rho_{i+1}^R}{s_{i+1}^R} + \frac{\rho_1^L}{s_1^L}, \tag{1.47}$$

for $i = 1, 2, \ldots$.

We can use these equations to solve for $\rho_i^L$ and $\rho_i^R$, in terms of $\rho_1^L$ and $\rho_1^R$. Moreover, the invariant density property for $\rho$ implies the associated measure

$$\mu_\rho(L_1) = \mu_\rho(R_1),$$

i.e.

$$\rho_1^L |L_1| = \rho_1^R |R_1|.$$

Thus the single unknown is reduced to one, say $\rho_1^L$. This of course can be found by using the fact that the probability density has $\mu_\rho([0, 1]) = 1$, and so

$$\sum_{i=1}^{\infty} (\rho_i^L |L_i| + \rho_i^R |R_i|) = 1.$$

### 1.6.3 Power-law escape

We can calculate the probability of 'escape' from an intermittency region. Specifically, we consider the probability of a sequence of $k$-consecutive zeroes for the output $s$ of an intermittency map $f$. We will consider the map

$$f(x) = \frac{x}{(1 - \hat{d}x^{m-1})^{\frac{1}{m-1}}},$$

for $0 \leq x \leq d$ and will assume a random injection to the region from $x > d$, [Pomeau & Manneville(1980)].

If the orbit re-enters the interval $[0, d]$ at the point $\bar{x}$, then that determines the sequence length $l$ of zeroes,namely, see section 1.6.1

$$k(x) = \frac{1}{\hat{d}} \left( \frac{1}{x^{(m-1)}} - \frac{1}{\bar{d}^{(m-1)}} \right). \tag{1.48}$$

So if $P(l)$ is the probability density for length $l$ zero sequences,

$$P(l)dl = P(l)\frac{dl}{dx}dx,$$

and then

$$\hat{P}(\bar{x}) = P(l(\bar{x}))\frac{dl}{d\bar{x}}$$

is the probability density for re-entry at the point $\bar{x}$.

If we are assuming the re-entry density $\hat{P}(\bar{x})$ to be uniform, then

$$P(l) = \left| \frac{d\bar{x}}{dl} \right| = \frac{1}{m-1} l^{-\frac{m}{m-1}},$$

a power law decay exponent $m/(m-1)$.

## 1.7 Auto-correlation

The average $E(G)$ of the function $G(x)$ with respect to an orbit $\{x_i\}_{i=1}^{\infty}$ is

$$\begin{aligned} E(G) &= \lim_{N\to\infty} \frac{1}{N} \sum_{i=1}^{N} G(x_i) \\ &= \lim_{N\to\infty} \frac{1}{N} \sum_{i=1}^{N} \int G(x)\delta(x - x_i)\, dx \\ &= \int G(x) \lim_{N\to\infty} \frac{1}{N} \sum_{i-1}^{N} \delta(x - x_i)\, dx \\ &= \int G(x)\rho(x)dx. \end{aligned} \tag{1.49}$$

We have already seen in Fig. 1.4 that the movement between strings of the output values '0' and '1' is rapid in the one and much slower than the second trace. The intermittency in one of the maps produces increased sojourn times for the two states. The longer sojourn times are said to introduce *memory* into the output which is reflected in higher correlation between the output binary sequence and the same sequence with a time-lag $k$. The *auto-correlation* vector of a sequence is the way in which the memory is measured.

Let $s_t$ be a scalar time series of the binary values $\{0, 1\}$ for $t = 0, 1, 2, \ldots$, and suppose the series is stationary. We define the auto-correlation of time lag $k$ by

$$\gamma(k) = \frac{E(X_t X_{t+k}) - E(X_t)E(X_{t+k})}{\sqrt{(}Var(X_t)Var(X_{t+k})).} \tag{1.50}$$

Let $\mu = E(X_t)$. Note that because the $X_t$ values are binary, $E(X_t^2) = E(X_t) = \mu$ and so $Var(X_t) = E(X_t^2) - E(X_t)^2 = \mu(1-\mu)$. Therefore, the auto-correlation can be re-written

$$\gamma(k) = \frac{E(X_t X_{t+k}) - \mu^2}{\mu(1-\mu)}. \tag{1.51}$$

Given $0 \leq X_t X_{t+k} \leq X_t$, it follows that $\gamma(k) \leq 1$. Note also that if there were no correlation, i.e. that the values $X_t$ were *independent* of each other, then $E(X_t X_{t+k}) = E(X_t)E(X_{t+k})$ and $\gamma(k) = 0$. Thus, in general, we expect that the correlation coefficient $\gamma(k)$ decays to zero. Two special types of decay are

(a) *power-law*, where $\gamma(k) \sim ck^{-\beta}$ for some constants $c$ and $\beta > 0$;

(b) *exponential decay*, where $\gamma(k) \sim c\alpha^{-k}$, for some constants $c$ and $\alpha > 0$.

Let us consider the correlation behaviour of the Bernoulli, or doubling, map $D$. The probability of the four transitions in one iteration

$$0 \to 0,\ 0 \to 1,\ 1 \to 0,\ 1 \to 1$$

by the map $D$ are each 0.25. Thus $E(X_t X_{t+1}) = 0.25(0 \cdot 0 + 0 \cdot 1 + 1 \cdot 0 + 1 \cdot 1) = 0.25$.

You can show similarly that more generally $E(X_t X_{t+k}) = 0.25$ for all $k > 0$. The uniform probability density in the interval $\mathbb{I}$ for the doubling map $D$ gives $E(X) = 0.5$. The time series $X_t$ is binary and so $X_t^2 = X_t$, which implies $E(X^2) = E(X)$. It follows that $\mathrm{Var}(X) = E(X^2) - E(X)^2 = E(X) - E(X)^2 = 0.5 - 0.5^2 = 0.25$. Therefore

$$\gamma(k) = \begin{cases} 1 & \text{for } k = 0 \\ (0.25 - 0.5^2)/0.25 = 0 & \text{for } k > 0. \end{cases} \tag{1.52}$$

### 1.7.1 Autocorrelation for intermittency maps

If we consider the piecewise linear maps constructed from two sequences $z_i = i^{-\alpha_1}$ at $x = 0$ and $w_i = 1 - i^{-\alpha_2}$ at $x = 1$, $\alpha_1, \alpha_2 > 1$, then the two intermittencies compete and it can be proven that

$$\gamma(k) \sim Kk^{-c}, \tag{1.53}$$

where

$$c = \text{Min}\{\alpha_1, \alpha_2\} - 1, \tag{1.54}$$

$K$ constant, [Barenco *et al*, 2004]. Thus the correlation for the composite map is determined by the heaviest tail in the correlation decay arising from the two competing intermittencies.

A similar result is also available for the differentiable case [Mondragon]. In this case, the map is

$$f(x) = \begin{cases} x + (1-d)\left(\frac{x}{d}\right)^{m_1} & 0 \le x < d \\ 1 - \left(\frac{1-x}{1-d}\right)^{m_2} & d \le x < 1. \end{cases} \tag{1.55}$$

with the extra condition that whenever $f$ iterates across the line $x = d$, the formula is replaced by a random uniform injection.

Allowing for change from the piecewise linear to the differentiable case, we have essentially the same result on the auto-correlation

$$\gamma(k) \sim K' k^{-c}, \tag{1.56}$$

where

$$c = (2-m)/(m-1), \tag{1.57}$$

$m = \text{Max}\{m_1, m_2\}$, $K'$ constant. It can be checked that the continuous-discrete transition $m_i = (1+\alpha_i)/\alpha_i$ (cf. eqn 1.46) converts the exponent $c$ in eqn 1.57 to the exponent for the discrete version in eqn 1.54, after noting $\text{Max}(m)$ corresponds to $\text{Min}(\alpha_i)$.

# Bibliography


[Barenco *et al*, 2004] Barenco M. & Arrowsmith D.K., The autocorrelation of double intermittency maps and the simulation of computer packet traffic , *Dynamical Systems*, **19**(1) 2004, 61-74.

[Coornaert & Papadopoulos(1993)] Coornaert M. & Papadopoulos A. 1993. Symbolic dynamics and Hyperbolic Groups. *Springer Verlag(Berlin & Heidelberg).*

[Crutchfield & Packard(1982)] Crutchfield J.P. & Packard N. 1982. Symbolic Dynamics of One-Dimensional Maps: Entropies, Finite Precision, and Noise. *Intl. J. Theo. Phys.* 21 433–466.

[Daw (1997)] Daw C. S., Finney C. E. A., Kennel M. B., & Connolly F. T. 1997. Cycle-by-cycle combustion variations in spark-ignited engines, *Proceedings of the Fourth Experimental Chaos Conference, Boca Raton, Florida USA.*

[Devaney(1986)] Devaney R.L. 1986. An Introduction to Chaotic Dynamical Systems. *Benjamin-Cummings.*

[Guckenheimer(1979)] Guckenheimer J. 1979. Sensitive dependence to initial conditions for one-dimensional maps. *Comm. Math. Phys.* 70 133–160.

[Guckenheimer (1977)] Guckenheimer J., Oster G. & Ipatchki A. 1977. The dynamics of density dependent population models. *Jnl Math. Biol.* 4 101–147.

[Hadamard (1898)] Hadamard J. 1898, Les surfaces á courbures opposeés e leur lignes géodesiques, *J.Math.Pures Appl.* 4 27–73.

[Hao (1989)] Hao B-L. 1986. Elementary Symbolic Dynamics and Chaos in Dissipative Systems. *World Scientific Publishing.*

[Hao & Zheng(1998)] Hao B-L & Zheng W-M. 1998 Applied Symbolic Dynamics and Chaos. *Directions in Chaos (7), World Scientific Publishing.*

[Hardy(1979)] Hardy. G.H. 1979. An Inroduction to the Theory of Numbers, *Oxford University Press*

[Mondragon] ondragon R. & Arrowsmith D.K., The random wall map, *preprint.*

[Lind & Marcus (1996)] Lind D. and Marcus B. 1996. An Introduction to Symbolic Dynamics and Coding. *Cambridge University Press.*

[Kitchens(1997)] Kitchens, B.P. Symbolic Dynamics; One-Sided, Two-Sided and Countable State Markov Shifts Series. *Universitext, Springer Verlag.*

[Milnor & Thurston(1988)] Milnor J. & Thurston W. 1988. On iterated maps of the interval. *Lect. Notes in Math.,in Dynamical Systems Proceedings, University of Maryland 1986-87 (J. C. Alexander, ed.) Springer-Verlag, Berlin)* 1342.

[Morse(1921)] Morse M. 1921. A one-to-one representation of geodesics on a surface of negative curvature, *American Journal of Mathematics* 43 33–51.

[Pomeau & Manneville(1980)] Pomeau Y., Manneville P., Intermittent transition to turbulence in dissipative dynamical systems, *Commun Math Phys* **74**, 1980, 189-197.

[Smale(1967)] Smale S. 1967, Differentiable Dynamical Systems, *Bulletin American Mathematical Society* 73(6) 747–817.

[Voss (2000)] Voss A., Wessel N., Kurths J., Schirdewan A., Osterziel K.J., Malik M.,Dietz R. 2000. Symbolic Dynamics - a Powerful Tool in Non-invasive Biomedical Signal Processing, *Advances in Noninvasive Electrocardiographic Monitoring Techniques. Kluwer Academic Publisher. Dordrecht (Eds: Osterhues H.H., Mombach V. Moss A.J.).* 429-437.